ECE diagnostic and -measurements during the first W7-X divertor campaign

M. Hirsch[1], U. Höfel[1], N. Chaudhary[1], A. Dinklage[1], J. Guerrero Arnaiz[1], N. Marushchenko[1], B. v. Milligen[2], J. W. Oosterbeek[1], T. Stange[1], J. Svensson[1], G. M. Weir[1], R.C. Wolf[1], M. Zanini[1] and the W7-X Team

[1] *Max-Planck-Institut f. Plasmaphysik, Greifswald, Germany*

[2] *Laboratorio Nacional de Fusion, CIEMAT, Avda. Complutense 40, 28040 Madrid, Spain*

The Electron Cyclotron Emission diagnostic (ECE) at W7-X is routinely operated to monitor ECR heating and electron heat transport. In its standard mode the diagnostic measures in 2nd harmonic extraordinary mode polarization (X2) in the frequency range from 126 to 162 GHz using a 32 channel radiometer with a single broadband mixer down to a detection frequency band between 4 and 40 GHz [1]. A Gaussian in-vessel optics defines the line-of-sight in the three dimensionally shaped stellarator plasma and maximizes spatial resolution by a slim beam waist < 23 mm all along the 55 cm passing the confinement region. For maintenance and daily access the radiometer is located outside the torus hall receiving the EC radiation via a circular 28mm diameter oversized transmission line of 24m length. A Michelson Interferometer sharing the same optics via a wire-grid splitter in the oversized transmission line is available for broadband spectra on a 45 ms time bases [2]. Both systems are protected against stray radiation from unabsorbed 140 GHz heating beams via notch filters.

1. ECE calibration

The 32 channel system is absolutely calibrated by means of a hot-cold source in front of an optics with identical geometry and -transmission line as the in-vessel optics but located outside the torus. A rotating mirror is used to chop between blackbody emitters at LN_2 and room temperature to cope with slow drifts of the system. After conditional averaging the desired radiometer response is derived from a Bayesian forward analysis with the graphics based framework MINERVA [3] including the full geometry of the calibration arrangement [4]. For daily tests and a drift characterization the receiver may be switched to a calibrated RF noise source launching into the oversized waveguide directly at the radiometer. The overall calibration factors derived for the individual radiometer channels vary by nearly two orders of magnitude decreasing towards higher detection frequencies. Main uncertainties of this ECE calibration result from slow (thermal) drifts of the channel sensitivities which for all channels prevail over the effect of the finite system noise during calibration. An improved temperature stabilization is being prepared. In contrast ECE signals during plasma operation

exceed those measured during calibration by five orders of magnitude such that the sytem noise is practically irrelevant for the measurement which gives access to fast plasma phenomena described below and allows for Te-profile inference on sub ms timescale.

2. ECE spectra and Te-profile inference

In W7-X as a result of its large aspect ratio the magnetic field gradients along the line-of-sight are moderate resulting in clearly separated cyclotron harmonics. The ECE spectra around the 2nd harmonic display the blackbody emission from the plasma core with high optical thickness but also downshifted emission from hot core electrons on the low-field (outboard) side [1]. The high-field- (inboard) side channels at the plasma boundary may already be hampered by downshifted 3rd harmonic emission. Inference of the local electron temperature profile $T_e(r)$ from the measured ECE radiation temperature spectra $T_{rad}(f)$ in a consistent way [5] requires the iterative use of the beam tracing with the radiation transport code TRAVIS and of equilibrium calculations with the VMEC-code. As a minimum required density information line-integrated density from the Dispersion Interferometer [6] is used as external input if Thomson scattering density profiles data are not available. The inference uses again forward modelling with the Bayesian analysis framework MINERVA with input profiles (priors) represented by Gaussian processes to minimize restrictions of profile shape by dedicated fitfunctions. Comparison of forward calculation and measured data is on the level of the ECE spectrum $T_{rad}(f)$, the respective priors - the $T_e(r)$ profiles - are derived from that. Profile inference may be performed at different levels of complexity and computational time: An initial guess using an estimate of the emiting layer via the cold resonance allows to separate non-themal components in the spectrum. Next the most probable $T_e(r)$ profile is derived from a Maximum-a-Posteriori approach, finally a Markov-Chain Monte-Carlo process allows to detemine the variety of compatible $T_e(r)$ profiles constituting the level of uncertainty in the knowledge of the $T_e(r)$ profile result. This analysis allows to extend the range of applicability beyond standard ECE cases in which the plasma is sufficiently black such that the ECE signals may be considered as T_e measurement from a narrow layer right behind the cold resonance. Already at moderate densities the ECE forward analysis provides a weak information on the density profile shape as well. With increasing density approaching and passing the X2 cut-off forward modelling of the ECE spectrum provides information of the density profile which may be used e.g. as a supplement or a cross calibration of Thomson scattering. The MINERVA frame allows easy extension to further diagnostic information - e.g. from other profile diagnostics - aiming on an integrated data analysis.

3. High-density ECE

W7-X developes high-density detached scenarios beyond the X2 cut-off ($n>n_{co}$(X2) = 1.2 10^{20} m^{-3}) heated solely by O2 ECRH [6,7] as a candidate for reactor relevant longpulse stellarator operation where no current related Greenwald limit exists. For such discharges the O2 ECE emission has been used successfully as a direct but uncalibrated control monitor for sufficient O2 heating beam absorption which is $\sim T_e^2$ and thus requires a minimum temperature. For continuous core temperature measurements beyond the X2 cut-off density ($n>n_{co}$(X2) = 1.2 10^{20} m^{-3}) the diagnostic capabilities of optically grey 3rd harmonic X3 is being investigated with the Michelson-Interferometer. It can be shown that already for medium densities where X2 ECE is available also the X3 emission has a sufficient optical thickness. This also allows for crosscalibration with X2 in a certain medium density range and an extension of ECE applicalbility to higher densities [8].

4. Dynamic Phenomena, Edge Pedestal and ELM-like transport activity

Various plasma dynamic phenomena have been studied comprising the effects of pellet injection, MHD phenomena, ECRH induced heatwaves [9] and ECCD driven fast temperature crashes [10], as well as spontaneous propagating Te-perturbations [11]. For example in dedicated magnetic "high-hiota" configurations where the 5/5 islands are slightly shifted into the confinement region and a 5/6 island separatrix occurs outside, prominent transport events are observed at the plasma boundary with a variety of diagnostics (Fig.1) [12,13]. Their characteristics are reminiscent to ELMs and it is speculated that they are related with the particular magnetic island structure [13]. The inversion radius of the transport events is around 200 to 400 eV, a cold-pulse propagates afterwards towards the plasma center. The events are rather unaffected by conditions deeper in the core such as improved core confinement scenarios. In case of pellet fuelling each pellet initiates an event, however, there are also events in-between the pellets. Already at the begin of the discharge, where the density is still increased by gas fueling, an 100 to 200 eV pedestal in the T_e profile builds up within 50 - 100 ms around 300eV until it is reduced by the first ELM-like event. Between events, the pedestal recovers to about the same value. The ECE spectra in Fig.2 are taken before this pedestal formation (blue) in the maximum of the pedestal (green) and in the Te minimum of the first crash. The pedestal contribution to electron confinement is small, although the overall confinement in these configurations is moderately improved [12].

Aknowledgment: This work has been carried out within the framework of the EUROfusion Consortium and has received funding from the Euratom research and training programme 2014-2018 and 2019-2010 under grant agreement number 633053. The views and opinions expressed herein do not necessarily reflect those of the European Commission.

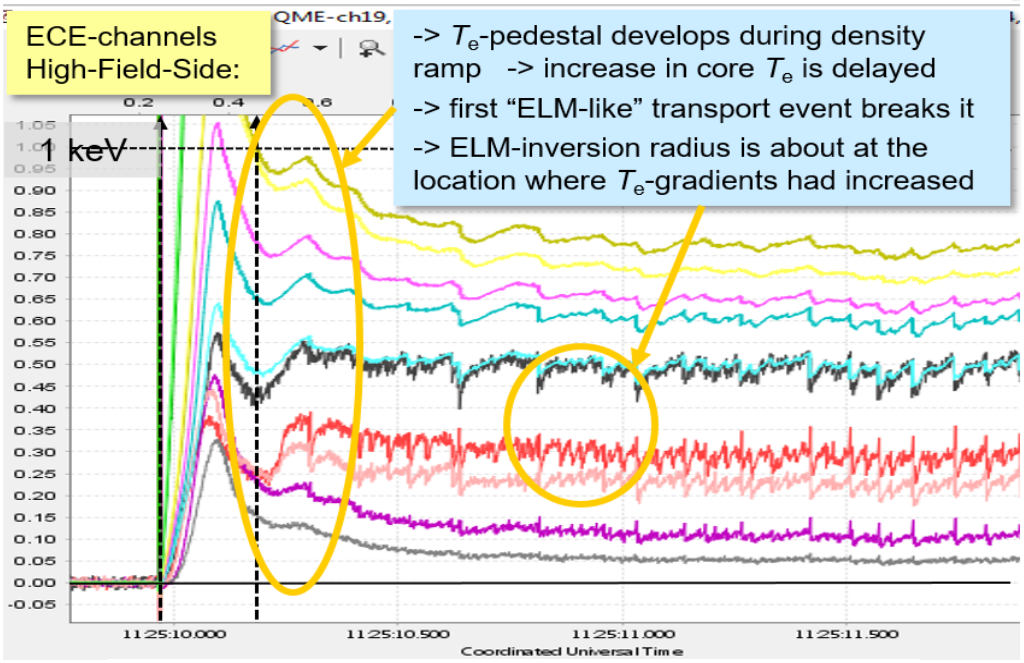

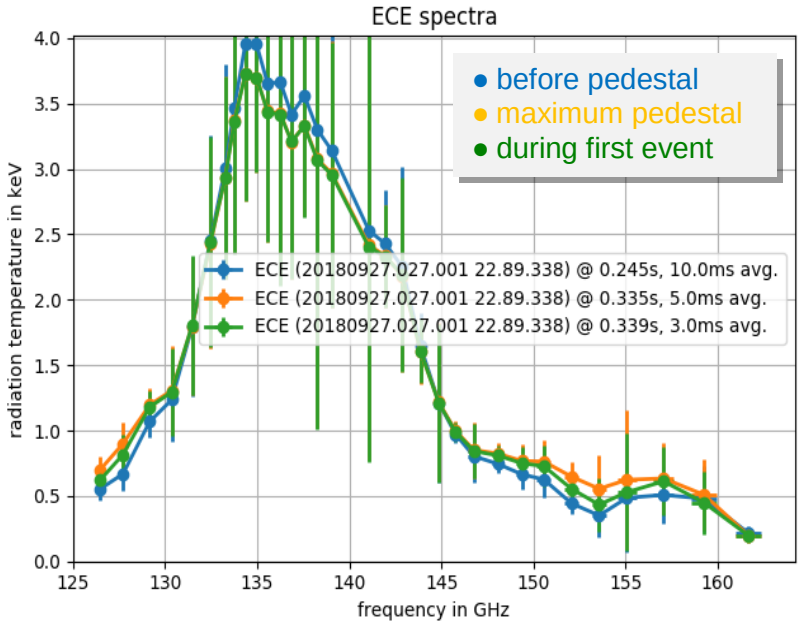

[1] M. Hirsch et al. EC20 2019 EPJ Web of Conferences 203, 03007
[2] H. Oosterbeek *et al.* 2019 *Fus. Eng. Des.*
[3] J. Svensson *et al.* 2011 *Contrib. Plasma Physics* Vol.51.2-3, p152-157
[4] U. Höfel *et al.* 2019 *Rev. Sci. Instrum.* 90, 043502
[5] U. Höfel *et al.* to be submitted to *Nucl. Fusion*
[6] K. J. Brunner *et al.* 2018 *JINST* 13 P09002
[7] R. Wolf *et al.* 2019 *Plasma Phys. Control. Fusion* 61 014037
[8] N. Chaudhary *et al.* this conference
[9] U. Höfel et al. 2016 Proc. of the 43rd EPS conf. on Plasma Physics P4.008
[10] M. Zanini *et al.* this conference
[11] B. Ph. van Milligen *et al.* 2018 *Nucl. Fusion* 58(7) 076002
[12] T. Andreeva *et al.* this conference
[13] G. Wurden *et al.* this conference